## General Disclaimer

## One or more of the Following Statements may affect this Document

- This document has been reproduced from the best copy furnished by the organizational source. It is being released in the interest of making available as much information as possible.

- This document may contain data, which exceeds the sheet parameters. It was furnished in this condition by the organizational source and is the best copy available.

- This document may contain tone-on-tone or color graphs, charts and/or pictures, which have been reproduced in black and white.

- This document is paginated as submitted by the original source.

- Portions of this document are not fully legible due to the historical nature of some of the material. However, it is the best reproduction available from the original submission.

NASA Technical Memorandum 83039



# Convergence Acceleration of Viscous Flow Computations

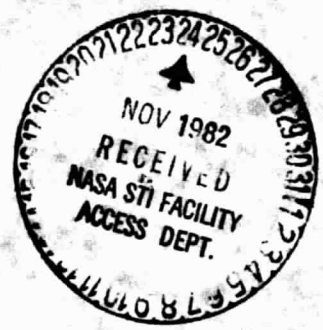


Gary M. Johnson
*Lewis Research Center*
*Cleveland, Ohio*

October 1982

NASA

# Convergence Acceleration of Viscous Flow Computations

Gary M. Johnson

National Aeronautics and Space Administration
Lewis Research Center
Cleveland, Ohio

## SUMMARY

A multiple-grid convergence acceleration technique recently introduced for application to the solution of the Euler equations by means of Lax-Wendroff algorithms is extended to treat compressible viscous flow.

Computational results are presented for the solution of the thin-layer version of the Navier-Stokes equations using the explicit MacCormack algorithm, accelerated by a convective coarse-grid scheme.

Extensions and generalizations are mentioned.

## INTRODUCTION

Ni (1981) introduced a multiple-grid convergence acceleration scheme for use with one-step Lax-Wendroff algorithms and applied it to the solution of the homoenthalpic Euler equations. Johnson (1982) extended this technique to the more general case of two-step Lax-Wendroff algorithms and illustrated its use, in conjunction with several members of this class, for the efficient solution of the full Euler equations. Of the two-step multiple-grid algorithms tested, all required substantially less work than Ni's original one-step method. The greatest efficiency was attained by accelerating the convergence of the MacCormack (1969) algorithm.

Although initial applications have focused on the Euler equations, the multiple-grid scheme presently under discussion may be employed with any hyperbolic system of conservation laws. Furthermore, it may be used to good advantage in accelerating the convergence of time-asymptotic solutions to viscous flow problems. Since such viscous flow computations are quite time-consuming, improvement in their efficiency is necessary in order to facilitate their use as design tools.

The present work discusses the extension of the multiple-grid convergence acceleration scheme for use in solving the Navier-Stokes equations. Two possibilities are described: the full coarse-grid scheme and the convective coarse-grid scheme. The full scheme is a straightforward application of previously-described principles to the Navier-Stokes system of conservation laws. The convective scheme is based on heuristic physical arguments and results in a

simplified procedure.

Results are presented for an application of the convective coarse-grid scheme, used with MacCormack's method, for the solution of the thin-layer version of the two-dimensional Navier-Stokes equations. The choices to use the thin-layer equations and to work in two dimensions were made for convenience and do not imply any restrictions inherent in the multiple-grid scheme. Extensions to three dimensions and to the full Navier-Stokes equations are conceptually clear and are reserved for future work.

## VISCOUS FLOW EQUATIONS

At present, the efficient numerical simulation of compressible flows by means of model equations based on the assumed existence of a velocity potential function is quite routine. More general inviscid flow problems may be modelled using the Euler equations. Efficient computational procedures for solving these equations are maturing rapidly. A limited range of viscous flows may be treated through a judicious combination of such inviscid models with correction procedures based on boundary layer theory. In the more general case, for example where the interaction between inviscid and viscous flow regions is no longer weak, the usual boundary layer approximations cannot be used. Here, the approach providing the greatest versatility is the use of the full Navier-Stokes equations, either in some sub-domain or in the entire flowfield.

### Navier-Stokes Equations

Following Peyret and Viviand (1975), the nondimensional Navier-Stokes equations may be written in conservation law form as

$$q_t = -(f_x + g_y) + Re^{-1}(r_x + s_y) \qquad (1)$$

where :

$$q = \begin{bmatrix} \rho \\ \rho u \\ \rho v \\ E \end{bmatrix} \qquad f = \begin{bmatrix} \rho u \\ \rho u^2+p \\ \rho uv \\ (E+p)u \end{bmatrix} \qquad g = \begin{bmatrix} \rho v \\ \rho uv \\ \rho v^2+p \\ (E+p)v \end{bmatrix}$$

$$r = \begin{bmatrix} 0 \\ \tau_{xx} \\ \tau_{xy} \\ \kappa Pr^{-1}(\gamma-1)^{-1}(a^2)_x + u\tau_{xx} + v\tau_{xy} \end{bmatrix} \qquad s = \begin{bmatrix} 0 \\ \tau_{xy} \\ \tau_{yy} \\ \kappa Pr^{-1}(\gamma-1)^{-1}(a^2)_y + u\tau_{xy} + v\tau_{yy} \end{bmatrix}$$

$$\tau_{xx} = (\lambda+2\mu)u_x + \lambda v_y$$

$$\tau_{xy} = \mu(u_y+v_x)$$

$$\tau_{yy} = (\lambda+2\mu)v_y + \lambda u_x$$

Here $\rho$, u, v, p, a and E are respectively density, velocity components in the x- and y- directions, pressure, sound speed and total energy per unit volume. The total energy per unit volume may be expressed as

$$E = \rho(e + \frac{1}{2}(u^2+v^2))$$

where the specific internal energy, e, is related to the pressure and density by the simple law of a calorically perfect gas

$$p = (\gamma-1)\rho e$$

with $\gamma$ denoting the ratio of specific heats. The coefficient of thermal conductivity, $\kappa$, and the viscosity coefficients, $\lambda$ and $\mu$, are assumed to be functions only of temperature. Furthermore, by invoking Stokes' assumption of zero bulk viscosity, $\lambda$ may be expressed in terms of the dynamic viscosity $\mu$ as

$$\lambda = -\frac{2}{3}\mu$$

Re and Pr denote the Reynolds and Prandtl numbers, respectively.

Although, for simplicity, the Navier-Stokes equations are presented here written in Cartesian coordinates, Viviand (1974) has shown that their strong conservation law form may be maintained under an arbitrary time-dependent transformation of coordinates. Explicit detail concerning the generalized coordinate version of these equations has been provided by Steger (1977) and need not be repeated here.

Thin-Layer Equations

The thin-layer approximation, in the words of Baldwin and Lomax (1978), "... evolves directly from a realistic assessment of what is really being computed in a typical high Reynolds number Navier-Stokes simulation." A highly stretched mesh is used to resolve the large flow gradients normal to the vorticity-generating surface. Consequently, because of limitations on computer capacity, the diffusion terms involving derivatives parallel to the surface are not resolved well enough to merit their computation.

Similar viscous terms are also neglected in the classical boundary layer approximation. However, while the boundary layer approximation replaces the normal momentum equation with the assumption that the normal pressure gradient is zero across the viscous layer, all momentum equations are retained in the thin-layer approximation and no assumptions are made concerning the pressure. Consequently, the separation point is not a singularity of the thin-layer model equations nor do the problems associated with matching a boundary layer solution to an inviscid outer flow occur when they are used.

In practice, the thin-layer assumption is implemented by using a body-fitted coordinate system and neglecting the viscous terms in the coordinate direction along the body. For Cartesian coordinates, with x representing the body-conforming coordinate, the thin-layer version of Eqn.(1) is

$$q_t = -(f_x + g_y) + Re^{-1} \tilde{s}_y \tag{2}$$

where :

$$\tilde{s} = \begin{bmatrix} 0 \\ \mu u_y \\ \frac{4}{3}\mu v_y \\ \kappa Pr^{-1}(\gamma-1)^{-1}(a^2)_y + \mu(uu_y + \frac{4}{3}vv_y) \end{bmatrix}$$

The extension of this assumption to generalized coordinates is straightforward and may be found in Steger (1977).

## FINE-GRID SOLUTION ALGORITHM

For convenience, Eqns.(1) and (2) may be rewritten as

$$q_t = -(F_x + G_y) \tag{3}$$

where, for the full Navier-Stokes equations,

$$F \equiv f - Re^{-1} r \qquad G \equiv g - Re^{-1} s$$

while, for the thin-layer equations,

$$F \equiv f \qquad G \equiv g - Re^{-1} \tilde{s}$$

An approximate numerical solution to Eqn.(3) may be computed by means of the two-step Lax-Wendroff algorithm introduced by MacCormack (1969). Having chosen a grid representative of the resolution desired in the converged solution, the forward predictor - backward corrector version of MacCormack's method may be written as

$$\Delta q_{i,j} = -\frac{\Delta t}{\Delta x}(F^n_{i+1,j} - F^n_{i,j}) - \frac{\Delta t}{\Delta y}(G^n_{i,j+1} - G^n_{i,j})$$

$$\delta q_{i,j} = -\frac{\Delta t}{2\Delta x}\left[ (F^n_{i+1,j} - F^n_{i,j}) + (\tilde{F}^{\gamma}_{i,j} - \tilde{F}^{\gamma}_{i-1,j}) \right] - \frac{\Delta t}{2\Delta y}\left[ (G^n_{i,j+1} - G^n_{i,j}) + (\tilde{G}^{\gamma}_{i,j} - \tilde{G}^{\gamma}_{i,j-1}) \right]$$

where :

$$\Delta q_{i,j} = \tilde{q}_{i,j} - q^n_{i,j}$$

$$\delta q_{i,j} = \left[ \; q(t+\Delta t) - q(t) \; \right]_{i,j}$$

$$\tilde{F}_{i,j} = F(\tilde{q}_{i,j})$$

$$\tilde{G}_{i,j} = G(\tilde{q}_{i,j})$$

First derivatives in the viscous terms are backward differenced in the predictor and forward differenced in the corrector.

This approach to solving viscous flow problems is quite robust and has been in widespread and successful use for some time, both for the time-accurate computation of unsteady flow and for the time-asymptotic solution of steady flow problems. In the latter case, where accurate resolution of physical transients is not required, the numerical stability limitation inherent in this explicit method may severely restrict the speed of its convergence to the steady state. Providing a method to accelerate convergence in this case is the object of this report.

## COARSE-GRID ACCELERATION SCHEME

Schemes of Lax-Wendroff type may be arrived at intuitively by using Taylor's theorem to write the approximation :

$$q(t+\Delta t) = q(t) + \Delta t q_t + \frac{\Delta t^2}{2} q_{tt} \tag{4}$$

Since we seek solutions to Eqn.(3), time derivatives may be expressed as space derivatives :

$$q_t = -(F_x + G_y)$$

$$q_{tt} = \left[ \; A(F_x + G_y) \; \right]_x + \left[ \; B(F_x + G_y) \; \right]_y$$

where A and B are the Jacobian matrices :

$$A \equiv \partial F/\partial q \qquad B \quad \partial G/\partial q$$

Substitution into Eqn.(4) results in :

$$q(t+\Delta t) = q(t) - \Delta t(F_x+G_y) + \frac{\Delta t^2}{2} \left\{ \left[ \; A(F_x+G_y) \; \right]_x + \left[ \; B(F_x+G_y) \; \right]_y \right\} \tag{5}$$

Second-order accurate spatial discretization of Eqn.(5) then yields a one-step Lax-Wendroff method.

For example, we may make the following finite-volume type approximations :

$$(F_x+G_y)_{i,j} = \frac{1}{8\Delta x}\left[ (F_{i+1,j+1} + 2F_{i+1,j} + F_{i+1,j-1}) - (F_{i-1,j+1} + 2F_{i-1,j} + F_{i-1,j-1}) \right] + \frac{1}{8\Delta y}\left[ (G_{i-1,j+1} + 2G_{i,j+1} + G_{i+1,j+1}) - (G_{i-1,j-1} + 2G_{i,j-1} + G_{i+1,j-1}) \right]$$

If we define the "change" in q at cell centers such that :

$$\Delta q_{i+\frac{1}{2},j+\frac{1}{2}} \equiv -\frac{\Delta t}{2\Delta x}\left[ (F_{i+1,j} + F_{i+1,j+1}) - (F_{i,j} + F_{i,j+1}) \right] - \frac{\Delta t}{2\Delta y}\left[ (G_{i,j+1} + G_{i+1,j+1}) - (G_{i,j} + G_{i+1,j}) \right] \tag{6}$$

it then follows that

$$-\Delta t(F_x+G_y)_{i,j} = \frac{1}{4}\left[ \Delta q_{i-\frac{1}{2},j-\frac{1}{2}} + \Delta q_{i-\frac{1}{2},j+\frac{1}{2}} + \Delta q_{i+\frac{1}{2},j+\frac{1}{2}} + \Delta q_{i+\frac{1}{2},j-\frac{1}{2}} \right] \tag{7}$$

Consistent with the above approximations and definition, we may write the approximation :

$$-\Delta t(F_x+G_y)_{i+\frac{1}{2},j+\frac{1}{2}} = \Delta q_{i+\frac{1}{2},j+\frac{1}{2}}$$

This motivates the definitions :

$$\Delta F_{i+\frac{1}{2},j+\frac{1}{2}} \equiv A_{i+\frac{1}{2},j+\frac{1}{2}}\, \Delta q_{i+\frac{1}{2},j+\frac{1}{2}}$$

$$\Delta G_{i+\frac{1}{2},j+\frac{1}{2}} \equiv B_{i+\frac{1}{2},j+\frac{1}{2}}\, \Delta q_{i+\frac{1}{2},j+\frac{1}{2}}$$

We then make the approximations :

$$-\Delta\tau \left\{ \left[ A(F_x+G_y) \right]_x \right\}_{i,j} =$$

$$\frac{1}{2\Delta x} \left[ \Delta F_{i+\frac{1}{2},j+\frac{1}{2}} + \Delta F_{i+\frac{1}{2},j-\frac{1}{2}} - \Delta F_{i-\frac{1}{2},j-\frac{1}{2}} - \Delta F_{i-\frac{1}{2},j+\frac{1}{2}} \right] \tag{8a}$$

$$-\Delta t \left\{ \left[ B(F_x+G_y) \right]_x \right\}_{i,j} =$$

$$\frac{1}{2\Delta y} \left[ \Delta G_{i+\frac{1}{2},j+\frac{1}{2}} + \Delta G_{i-\frac{1}{2},j+\frac{1}{2}} - \Delta G_{i-\frac{1}{2},j-\frac{1}{2}} - \Delta G_{i+\frac{1}{2},j-\frac{1}{2}} \right] \tag{8b}$$

If we now define the "correction" to q at grid nodes :

$$\delta q_{i,j} \equiv \left[ q(t + \Delta t) - q(t) \right]_{i,j}$$

we may combine Eqns.(7) and (8) to yield :

$$\begin{aligned} \delta q_{i,j} = & \frac{1}{4} \left[ \Delta q + \frac{\Delta t}{\Delta x}\Delta F + \frac{\Delta t}{\Delta y}\Delta G \right]_{i-\frac{1}{2},j-\frac{1}{2}} \\ & + \frac{1}{4} \left[ \Delta q + \frac{\Delta t}{\Delta x}\Delta F - \frac{\Delta t}{\Delta y}\Delta G \right]_{i-\frac{1}{2},j+\frac{1}{2}} \\ & + \frac{1}{4} \left[ \Delta q - \frac{\Delta t}{\Delta x}\Delta F - \frac{\Delta t}{\Delta y}\Delta G \right]_{i+\frac{1}{2},j+\frac{1}{2}} \\ & + \frac{1}{4} \left[ \Delta q - \frac{\Delta t}{\Delta x}\Delta F + \frac{\Delta t}{\Delta y}\Delta G \right]_{i+\frac{1}{2},j-\frac{1}{2}} \end{aligned} \tag{9}$$

Eqns.(6) and (9) constitute the one-step Lax-Wendroff method used as a basic integration scheme by Ni (1981). He gives the following heuristic interpretation to these equations : the first calculates the change in q occurring in a control volume during the increment $\Delta t$ while the second distributes the effects of the changes occurring in four nearest-neighbor control volumes to their common central nodal point where they are combined to form the correction to the vector of conservation variables, as illustrated in Fig. 1. This interpretation motivates the construction of the coarse-grid acceleration scheme.

## Full Coarse-Grid Scheme

Given the fine-grid corrections, which may be computed by any one- or two-step Lax-Wendroff scheme, as shown in Johnson (1982), we wish to use successively coarser grids to propagate these corrections throughout the computational domain, thus accelerating convergence to the steady state while maintaining the accuracy determined by the fine-grid discretization. Given a basic fine grid with the number of points in each direction expressible as $2^p + 1$ for p a natural number, let successively coarser grids be defined by successive deletion of every other point in each coordinate direction. The full coarse-grid acceleration scheme, as illustrated in Fig. 2, then replaces the computation of coarse grid changes by Eqn.(6) with a restriction of the latest fine-grid correction. This restricted fine-grid correction is then distributed according to a coarse-grid version of Eqn.(9) to obtain a coarse-grid correction which is, in turn, prolonged to the fine grid to become the new fine-grid correction. One time-cycle of the multiple-grid scheme is composed of an application of some Lax-Wendroff scheme on the fine grid followed by an application of the coarse-grid solution procedure to each successively coarser grid. The flow of information in this process is depicted in Fig. 3.

In the basic integration scheme, a change at one grid point affects only its nearest neighbors while, in a k-level multiple grid scheme, the same change affects all points up to $2^{k-1}$ mesh spacings distant. Furthermore, since the change is always determined by information from the fine grid and simply propagated by the distribution formulae for coarser grids, fine grid accuracy is maintained.

## Convective Coarse-Grid Scheme

The multiple-grid convergence acceleration procedure using the full coarse-grid scheme is essentially that described in Johnson (1982) for use with the Euler equations, with the Jacobian matrices of the flux vectors replaced by their appropriate viscous counterparts.

Consideration of the physical processes being modelled in a viscous flow computation leads to the formulation of an alternative coarse-grid scheme. Dissipative effects have a local character and their influence need not be taken into account in the construction of coarse-grid distribution formulae. Rather, it is the convective terms, with their global character, which are the key element in coarse-grid propagation. Hence, a coarse-grid scheme for viscous flow computations may be formulated on the basis of the inviscid equations of motion. Such a convective coarse-grid scheme is inherently more efficient than the full coarse-grid scheme because of the diminished computational effort associated with forming the Jacobian matrices of the Euler flux vectors rather than those of the viscous flux vectors. An additional benefit is that the convective coarse-grid scheme leads to a multiple-grid convergence acceleration procedure which is independent of the nature of the dissipative terms retained in the viscous model equations. That is to say that the coarse-grid scheme used previously for the Euler equations may be employed, without modification, to accelerate the convergence of viscous flow computations based on the Navier-Stokes equations, the thin-layer equations, or any other viscous model equations which contain the full inviscid Euler equations.

The correctness of the heuristic physical reasoning used in the formulation of the convective coarse-grid scheme is verified by the computational results presented below.

## RESULTS

We illustrate the use of multiple-grid convergence acceleration in viscous flow computations by means of a mathematically and physically simple example. We use MacCormack's method as a fine-grid solution algorithm for the thin-layer version of the Navier-Stokes equations and accelerate its convergence to a steady solution with the convective coarse-grid scheme.

We consider the subsonic flow through a cascade of unstaggered flat plates at zero angle of attack, as illustrated in Fig. 4. The ratio of exit static pressure to upstream total pressure is 0.8430191, yielding flow Mach numbers in the vicinity of 0.5 for the test cases to be exhibited here. The Reynolds numbers, based on cascade gap and critical speed, span the approximate range from $8.4 \times 10^3$ to $2.0 \times 10^5$. Symmetry is invoked to limit the size of the computational domain and the flow is assumed to be laminar. These assumptions are made for convenience in specifying the number and location of fine-grid nodal points and do not imply limitations on the generality of the method.

The choice of boundary conditions is also indicated in Fig. 4. At the inlet, total temperature, total pressure and flow angle are fixed, while at the exit, only the static pressure is specified. Along the plate surface the no-slip condition is applied and the temperature is specified. Along the remaining boundary sections the tangency condition is used. Uniform flow at the isentropic Mach number implied by the ratio of exit static pressure to inlet total pressure is used as an initial state. The values of the dependent variables on the domain boundaries are updated only during the fine-grid computations. This decouples the coarse-grid acceleration scheme from the details of boundary condition implementation.

As illustrated in Fig. 5, three different fine grids are employed in this study. All have the same number of nodal points and have their transverse grid lines located at the same positions. They differ in the positioning of their lateral grid lines. These are smoothly stretched away from the solid boundary in a geometric progression, starting from the initial spacings indicated in Fig. 5. These fine grids each allow the construction of four successively coarser grids, as indicated in Table I. The members of these grid families may then be used in combination to form multiple-grid sequences of length one through five.

Computations have been performed for the combinations of Reynolds number and fine grid configuration indicated in Table II. Isomach contours for the converged solutions produced for each case are shown in Fig. 6. The contour levels displayed are not equally spaced and are the same for all five cases shown. Nevertheless, they provide a good qualitative indication of the nature of the computed flowfields. More quantitative information is contained in Fig. 7, where normalized u-velocity profiles are illustrated. Here, the u-velocity, normalized with its value at the top boundary and same streamwise station, is plotted as a

function of relative distance from the bottom boundary. Curves for every second streamwise station, starting with the plate leading edge and ending at the outflow boundary, are displayed. They are staggered in proportion to the spacing of their respective streamwise stations. The data displayed in Figs. 6 and 7 are for conditions of optimal work reduction, as indicated in Table II. However, in each case the solution obtained is not a function of grid sequence length. This was verified by extensive computational experimentation.

Convergence histories are shown in Fig. 8. For each case, we display the fine grid convergence history and the corresponding convergence history for that grid sequence length which produced the best work reduction factor. Several of the plots have been truncated to fit within the residual range displayed.

For all five test cases and the five possible grid sequence lengths, the computational work required to reduce a standard error measure to a specified tolerance has been recorded. In each case, based on these data, we may estimate a work reduction factor and a corresponding optimal multiple-grid sequence length. Here we define the work reduction factor to be that multiple by which the work required to produce a converged solution using a single fine grid exceeds the work required to produce the same result using that multiple-grid sequence length which minimizes the computational work. The results obtained are recorded in Table II. Work reduction factors ranging from 1.5 to 4.8 have been realized. We observe that while the work reduction factor and, possibly, the optimal grid sequence length decrease with increasing grid stretching, they do not appear to decrease with increasing Reynolds number.

Several issues bearing on the multiple-grid work reduction factor should be mentioned at this juncture. When one considers convergence acceleration of the turbulent full Navier-Stokes equations, greater work reduction than obtained here will result by virtue of the inclusion of the full viscous terms and turbulence modelling on the fine grid. The treatment of the Jacobian matrices used in the coarse-grid acceleration scheme has a large influence on the efficiency of the coarse-grid computations, and hence, on the work reduction factor. Substantial improvement appears to be possible over the current treatment of these Jacobians. In the present computations, injection is used as the restriction operator and linear interpolation is chosen as the prolongation operator. These choices may not be optimal for use on highly stretched grids. Better choices could increase both the optimal grid sequence length and the work reduction factor. Similar consequences might result from an alternative coarse-grid formation strategy.

Given the encouraging results obtained to date, more comprehensive testing and more sophisticated applications of the viscous flow convergence acceleration ideas presented here are planned.

## CONCLUSIONS

Two coarse-grid schemes for use in the multiple-grid convergence acceleration of viscous flow computations have been presented : the full coarse-grid scheme and the simpler and more efficient convective coarse-grid scheme.

The convective coarse-grid scheme is of quite general applicability and may be used without modification with any model equations in the hierarchy ranging from the Euler equations to the full Navier-Stokes equations.

Computational evidence of the utility of the present approach to convergence acceleration has been provided by using the convective coarse-grid scheme, in conjunction with MacCormack's two-step Lax-Wendroff method, to solve the thin-layer version of the Navier-Stokes equations for a simple model problem.

Work reduction factors ranging from 1.5 to 4.8 have been obtained in initial testing over a fairly broad range of Reynolds numbers and grid stretchings.

More comprehensive testing and more sophisticated applications, including extension of the techniques discussed here to three dimensions, are planned.

## REFERENCES


Baldwin, B.S. and Lomax, H.: Thin-Layer Approximation and Algebraic Model for Separated Turbulent Flows. AIAA Paper 78-257, Jan. 1978.

Johnson, G.M.: Multiple-Grid Acceleration of Lax-Wendroff Algorithms. NASA TM-82843. Mar. 1982.

MacCormack, R.W.: The Effect of Viscosity in Hypervelocity Impact Cratering. AIAA Paper 69-354, Apr. 1969.

Ni, R.H.: A Multiple Grid Scheme for Solving the Euler Equations. AIAA Paper 81-1025, June 1981.

Peyret, R. and Viviand, H.: Computation of Viscous Compressible Flows Based on the Navier-Stokes Equations. AGARD AG-212, Sep. 1975.

Steger, J.L.: Implicit Finite Difference Simulation of Flow About Arbitrary Geometries with Application to Airfoils. AIAA Paper 77-665, June 1977.

Viviand, H.: Formes Conservatives des Équations de la Dynamique des Gaz. La Recherche Aérospatiale, No.1, Jan.-Feb. 1974, pp. 65-66.

TABLE I. - GRID DESCRIPTIONS

| Grid | 1 | 2 | 3 | 4 | 5 |
|---|---|---|---|---|---|
| Number of Points | 65 x 33 | 33 x 17 | 17 x 9 | 9 x 5 | 5 x 3 |

TABLE II. - ALGORITHM EFFICIENCY

| Test Case | Reynolds Number | Initial Transverse Spacing | Optimal Sequence Length | Work Reduction Factor |
|---|---|---|---|---|
| a | $8.4 \times 10^3$ | 0.0125 | 5 | 4.8 |
| b | $8.4 \times 10^3$ | 0.00625 | 3 | 2.7 |
| c | $3.4 \times 10^4$ | 0.00625 | 2 or 3 | 3.0 |
| d | $3.4 \times 10^4$ | 0.0025 | 2 or 3 | 1.5 |
| e | $2.0 \times 10^5$ | 0.0025 | 3 | 1.8 |

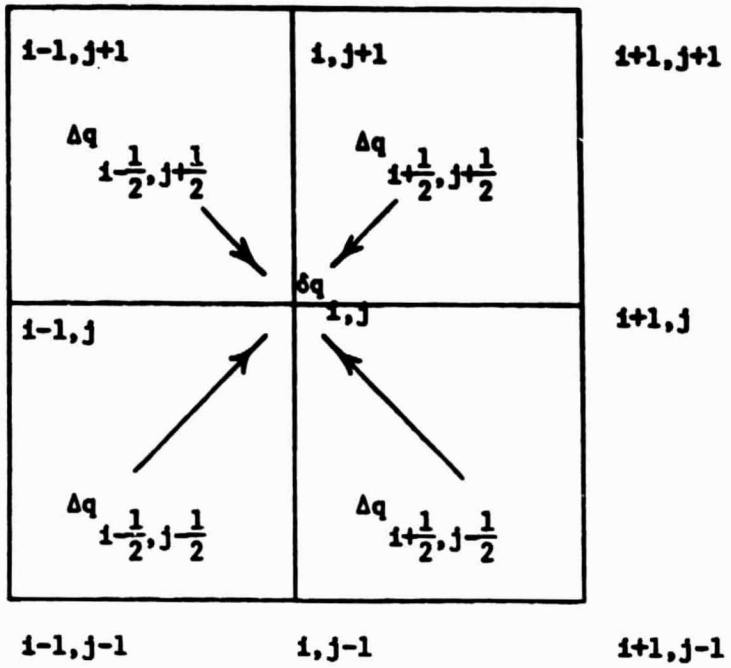


FIGURE 1. - One-Step Lax-Wendroff Scheme

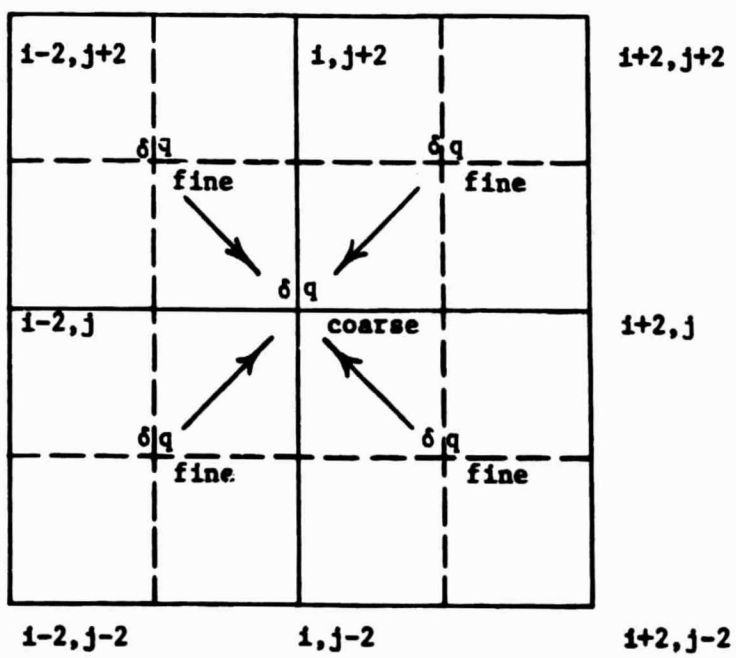


FIGURE 2. - Coarse Grid Scheme

R - Restriction of Latest Fine-Grid $\delta q$ as Coarse-Grid $\Delta q$

P - Prolongation of Coarse-Grid $\delta q$ to Fine Grid

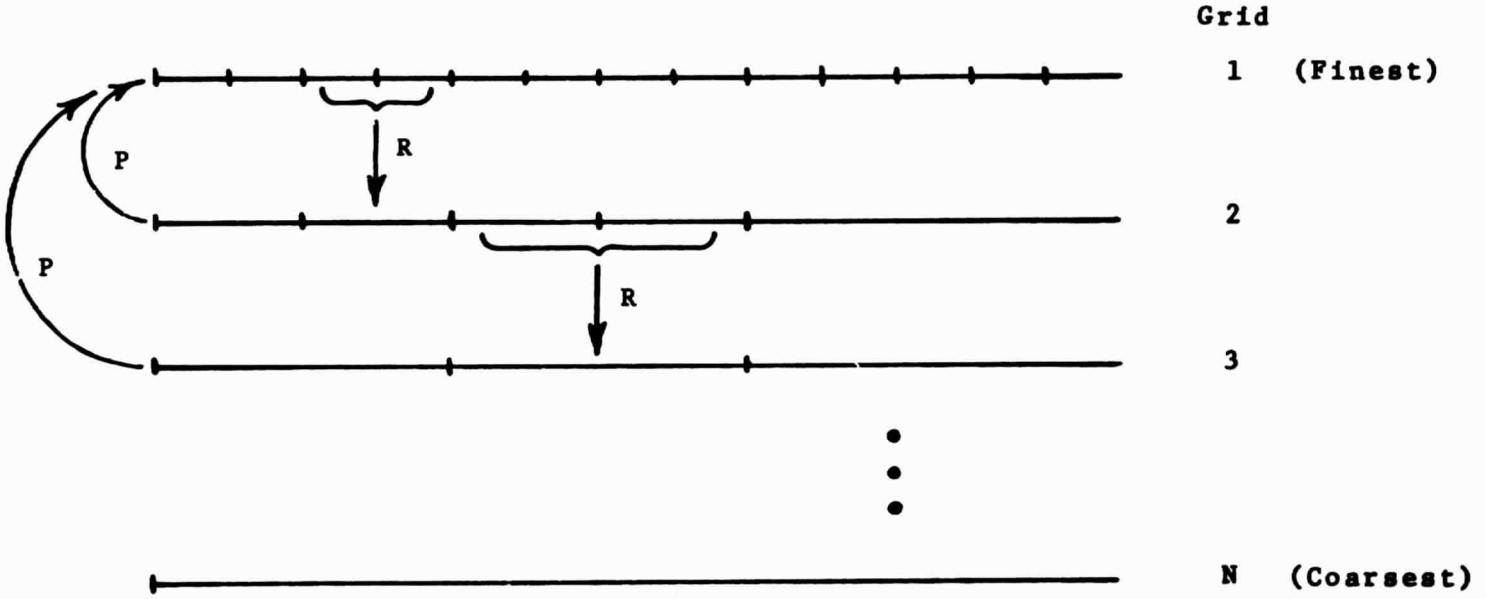


FIGURE 3. - Multiple-Grid Information Flow

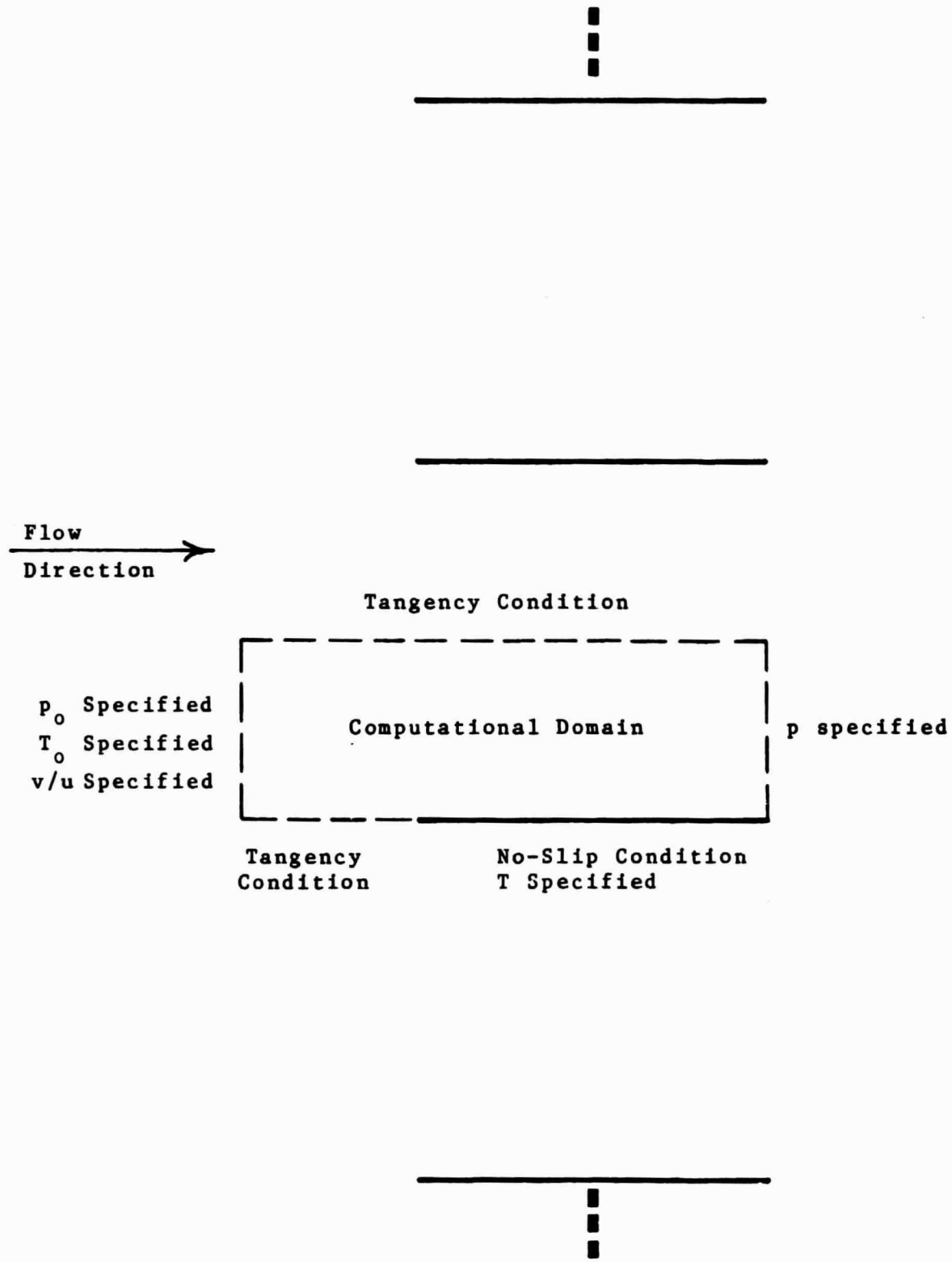


FIGURE 4. - Physical Problem

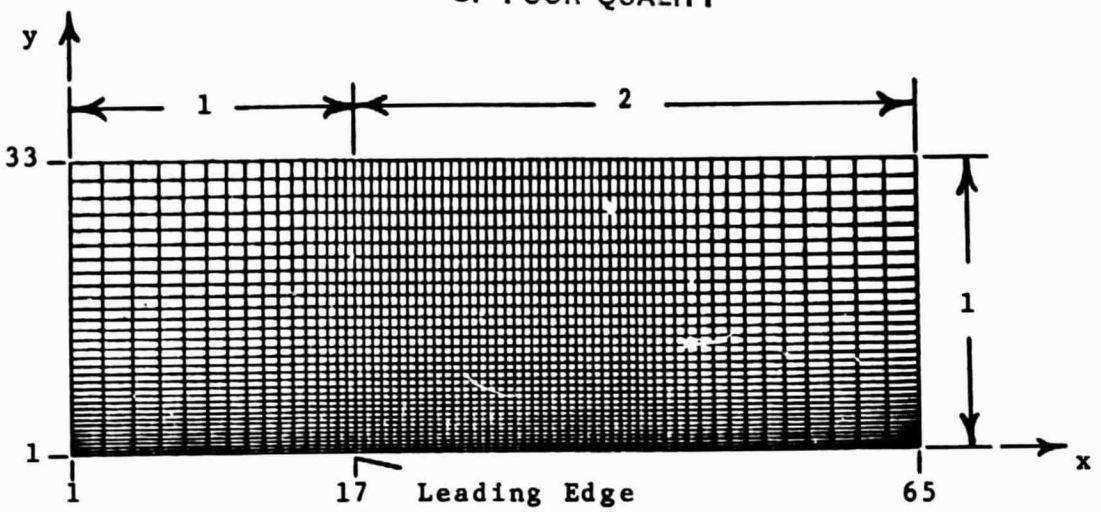


Smallest Grid Spacing : $\Delta x = 0.03125$
$\Delta y = 0.0125$

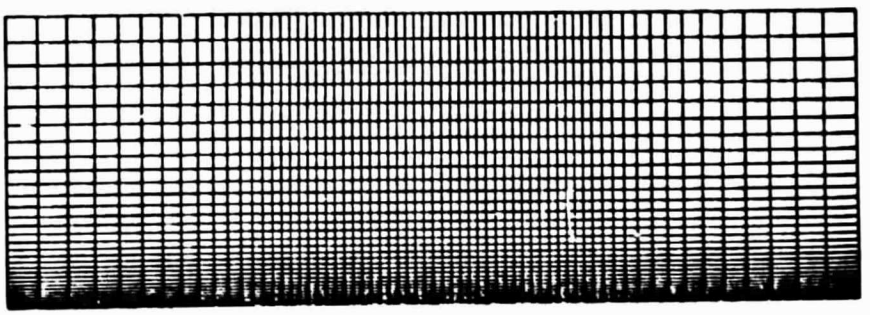

Smallest Grid Spacing : $\Delta x = 0.03125$
$\Delta y = 0.00625$

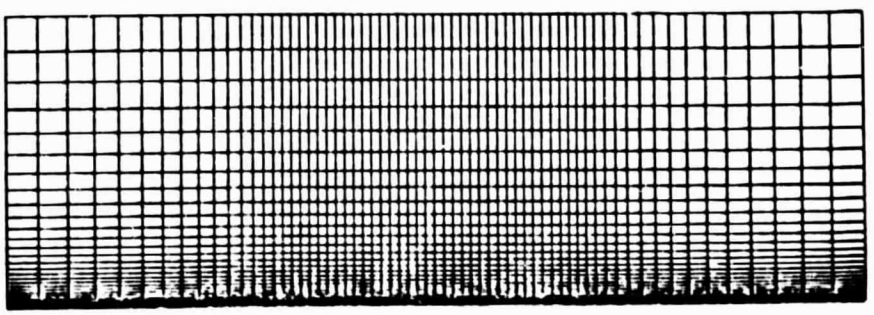

Smallest Grid Spacing : $\Delta x = 0.03125$
$\Delta y = 0.0025$

FIGURE 5. - Fine Grid Configurations

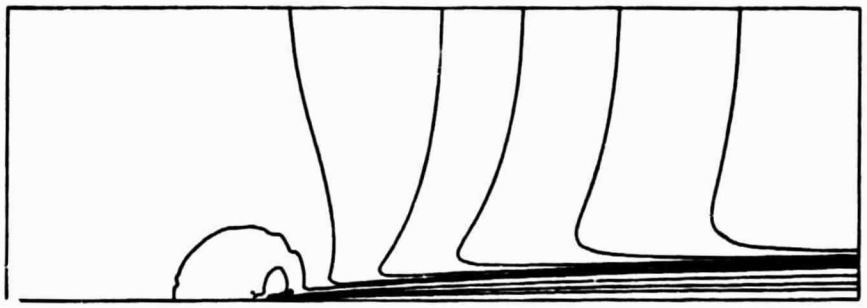

FIGURE 6a. - Isomach Contours
$Re = 8.4 \times 10^3$ , $\Delta y = 0.0125$

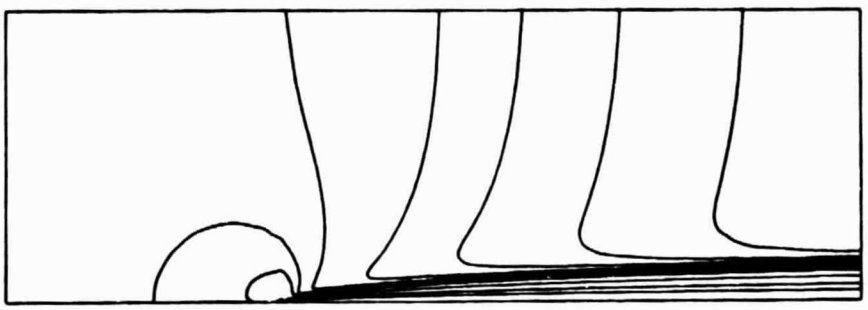

FIGURE 6b. - Isomach Contours
$Re = 8.4 \times 10^3$ , $\Delta y = 0.00625$

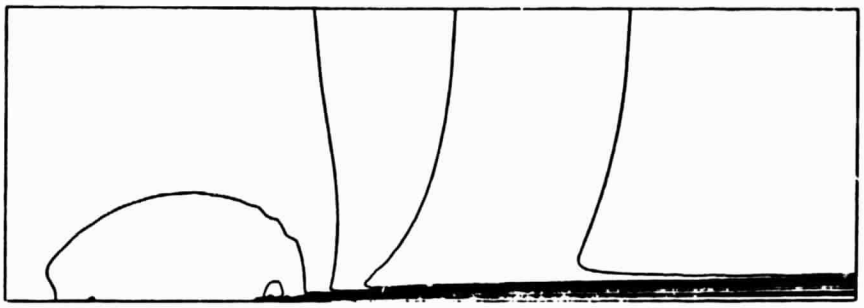

FIGURE 6c. - Isomach Contours
Re = 3.4 x $10^4$ , $\Delta y$ = 0.00625

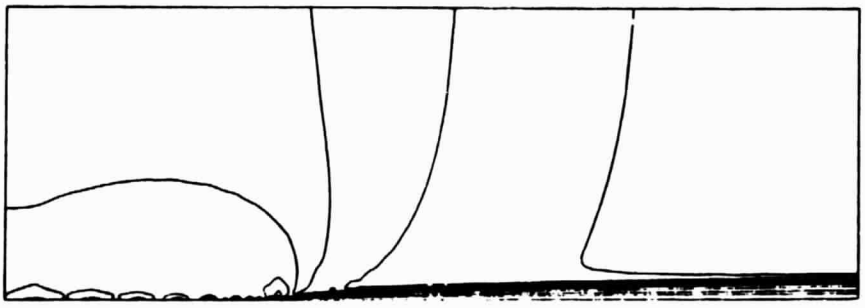

FIGURE 6d. - Isomach Contours
Re = 3.4 x $10^4$ , $\Delta y$ = 0.0025

FIGURE 6e. - Isomach Contours
$Re = 2.0 \times 10^5$ , $\Delta y = 0.0025$

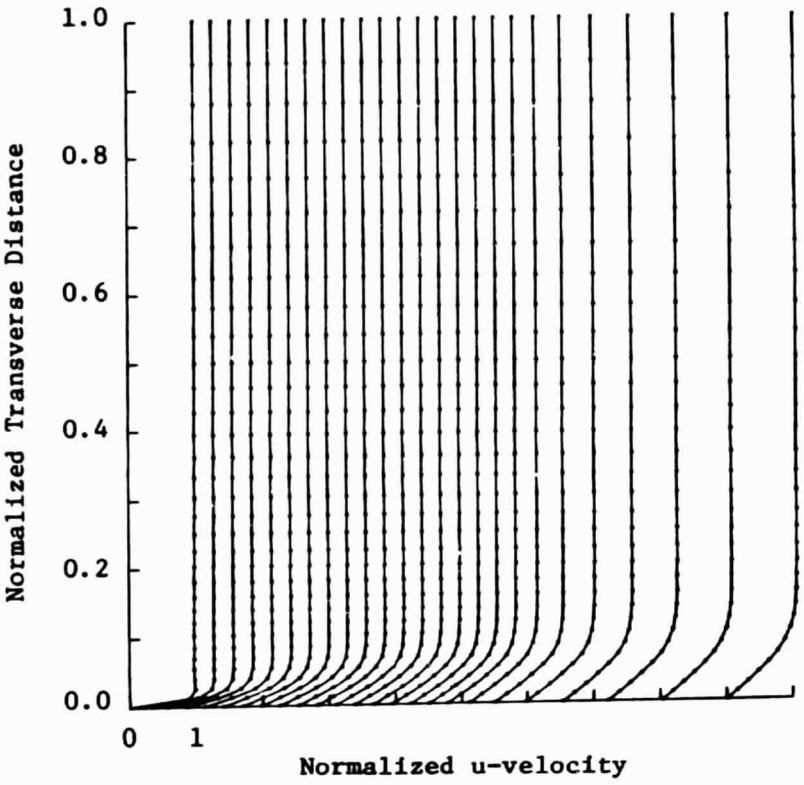


FIGURE 7a. - Velocity Profiles
Re = 8.4 x $10^3$ , $\Delta y$ = 0.0125

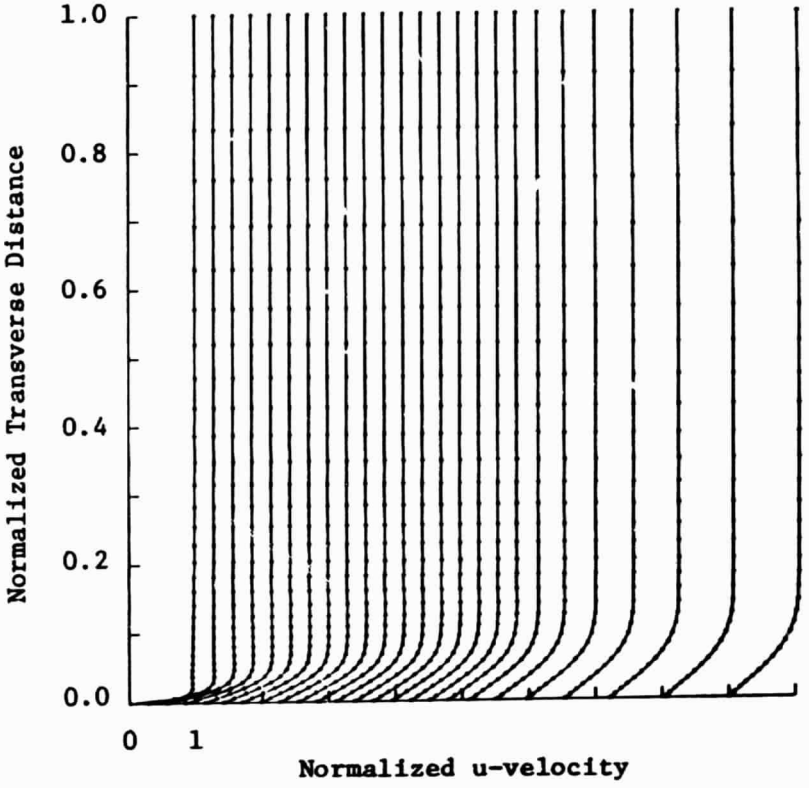


FIGURE 7b. - Velocity Profiles
Re = 8.4 x $10^3$ , $\Delta y$ = 0.00625

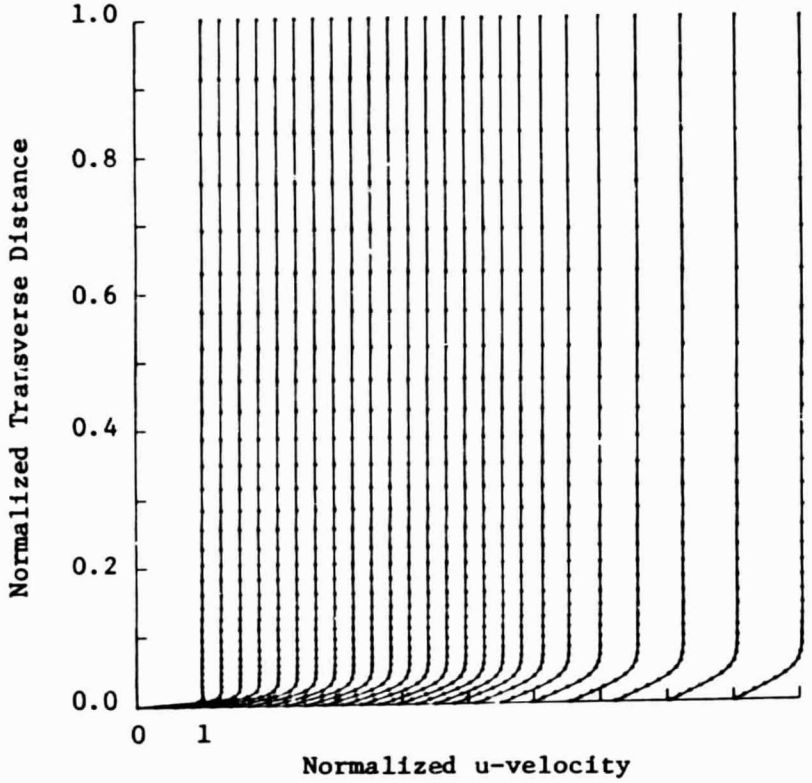


FIGURE 7c. - Velocity Profiles
Re = 3.4 x $10^4$ , $\Delta y$ = 0.00625

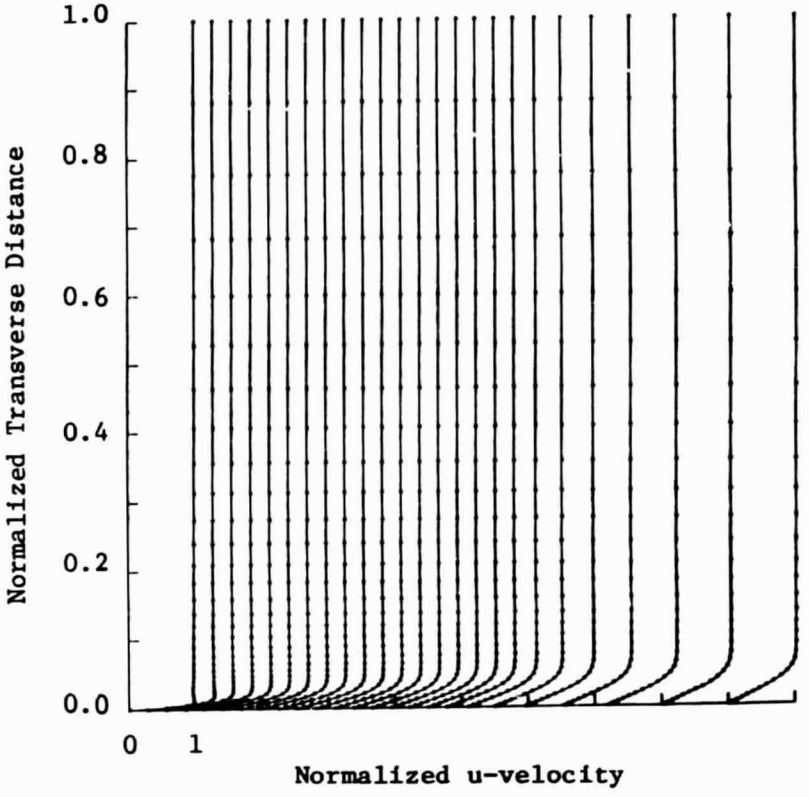




FIGURE 7d. - Velocity Profiles
Re = 3.4 x $10^4$ , $\Delta y$ = 0.0025

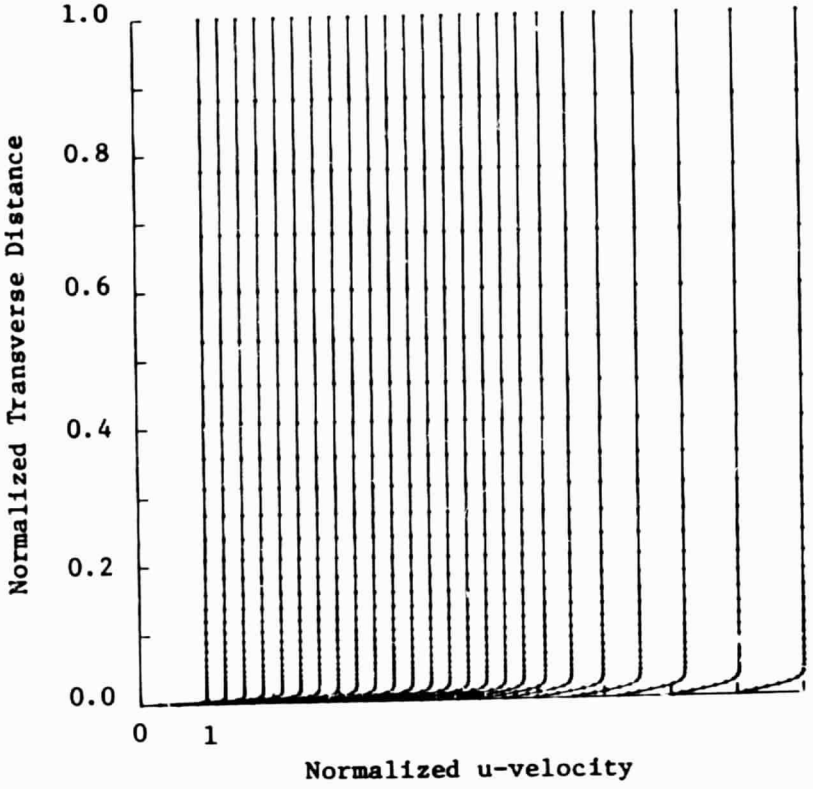


FIGURE 7e. - Velocity Profiles
$Re = 2.0 \times 10^5$ , $\Delta y = 0.0025$

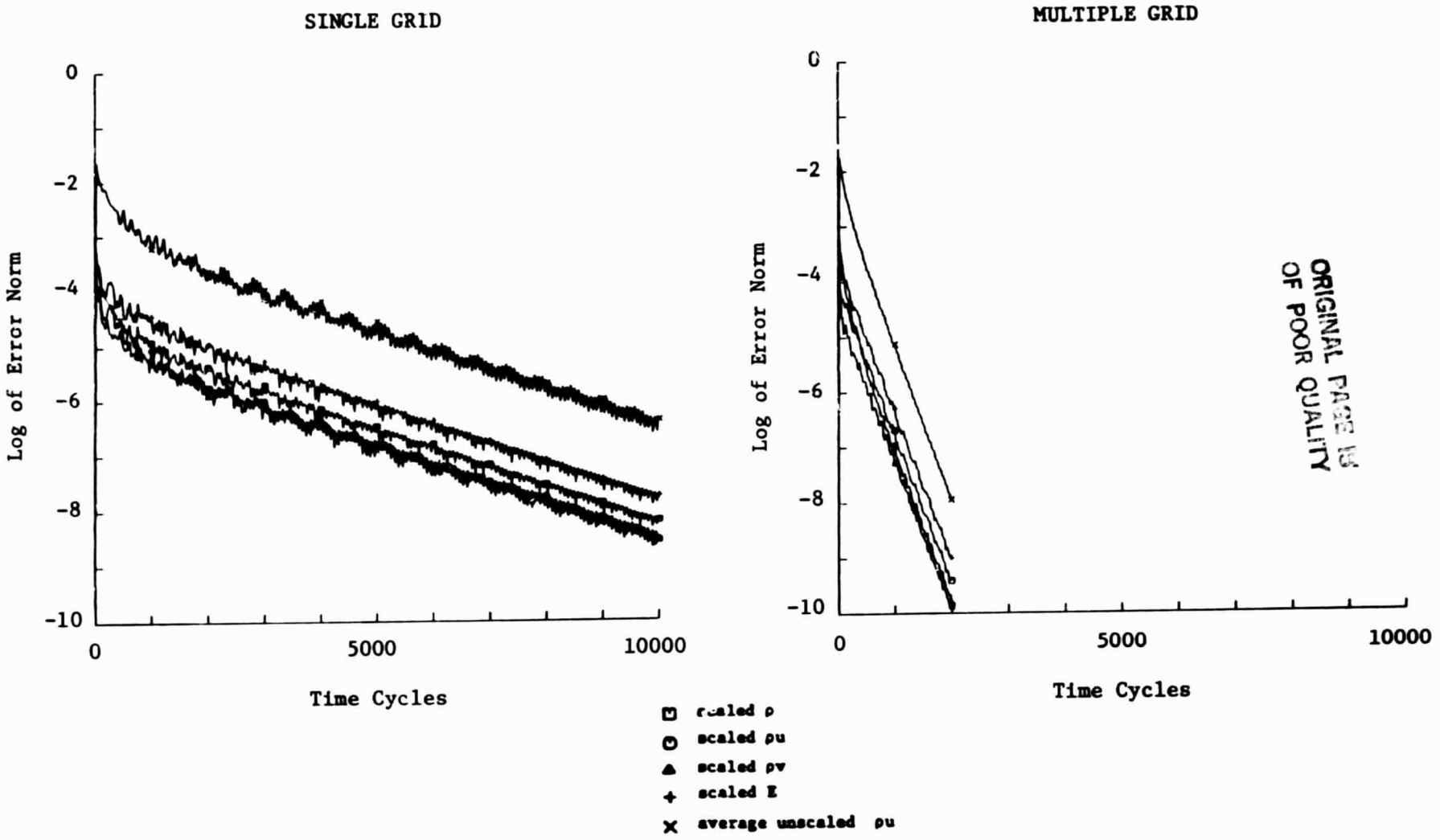


FIGURE 8a. - Convergence Histories

$Re = 8.4 \times 10^3$ , $\Delta y = 0.0125$

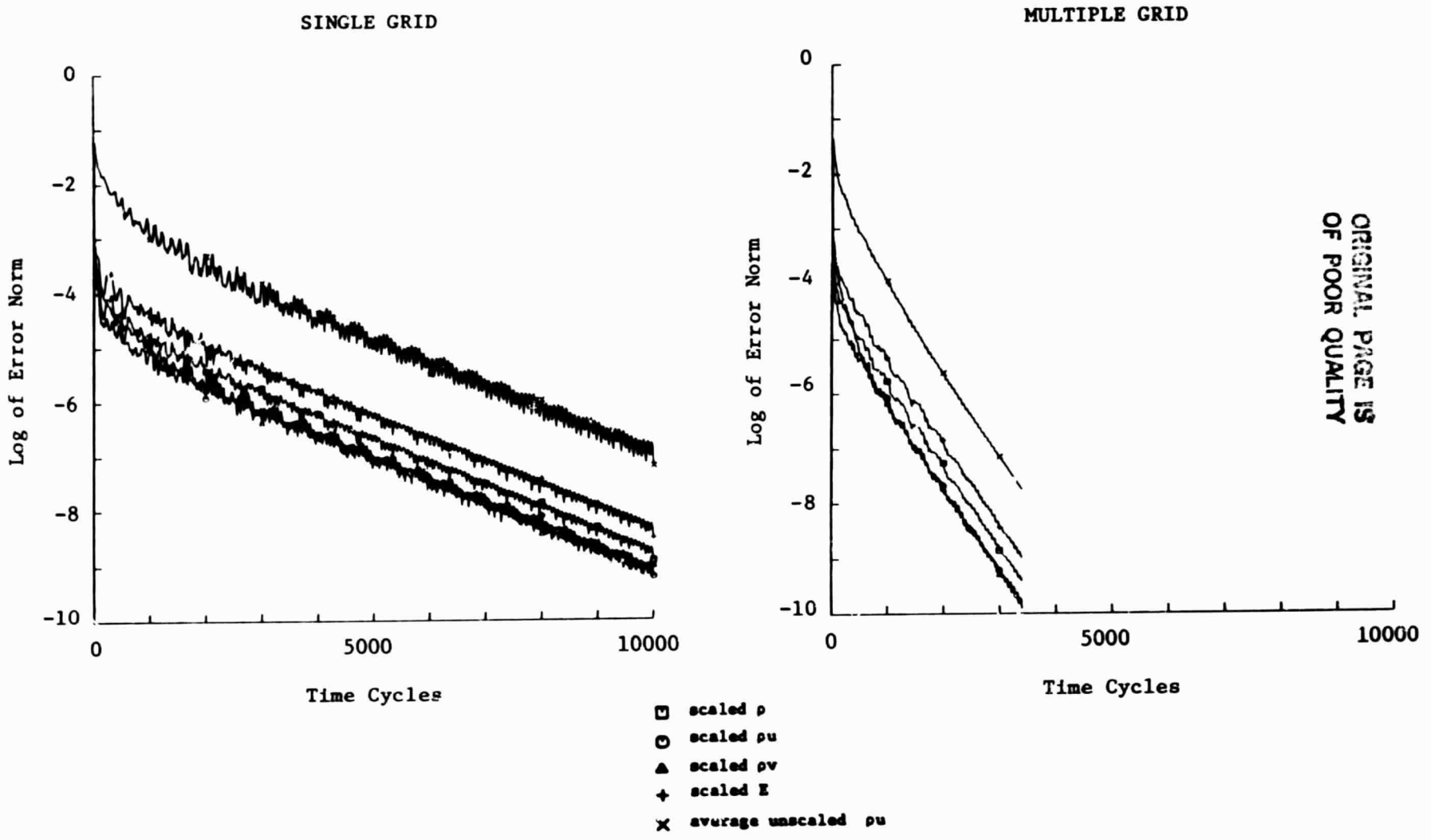




FIGURE 8b. - Convergence Histories

$Re = 8.4 \times 10^3$ , $\Delta y = 0.00625$

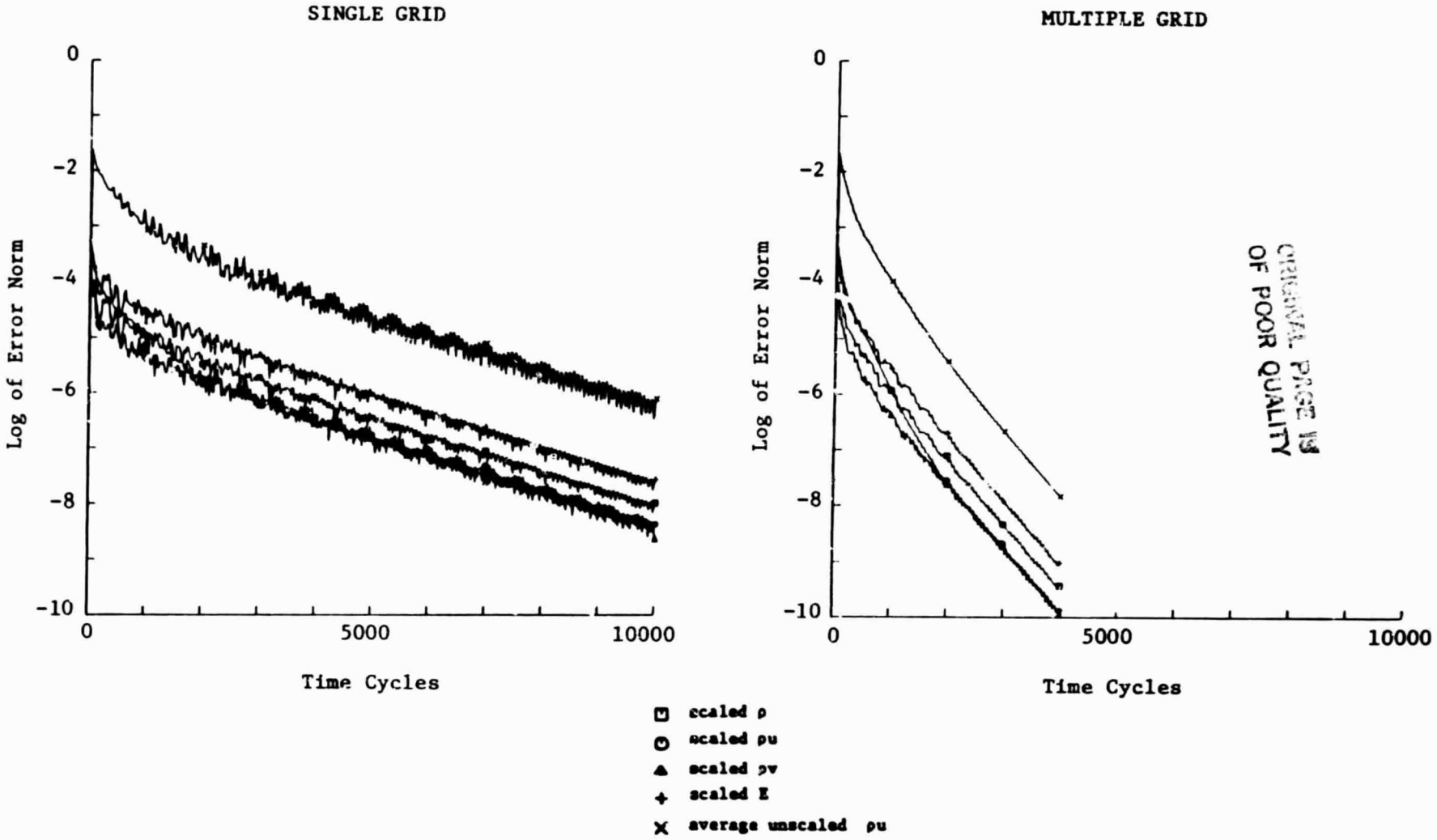




FIGURE 8c. - Convergence Histories

Re = 3.4 x $10^4$ , $\Delta y$ = 0.00625

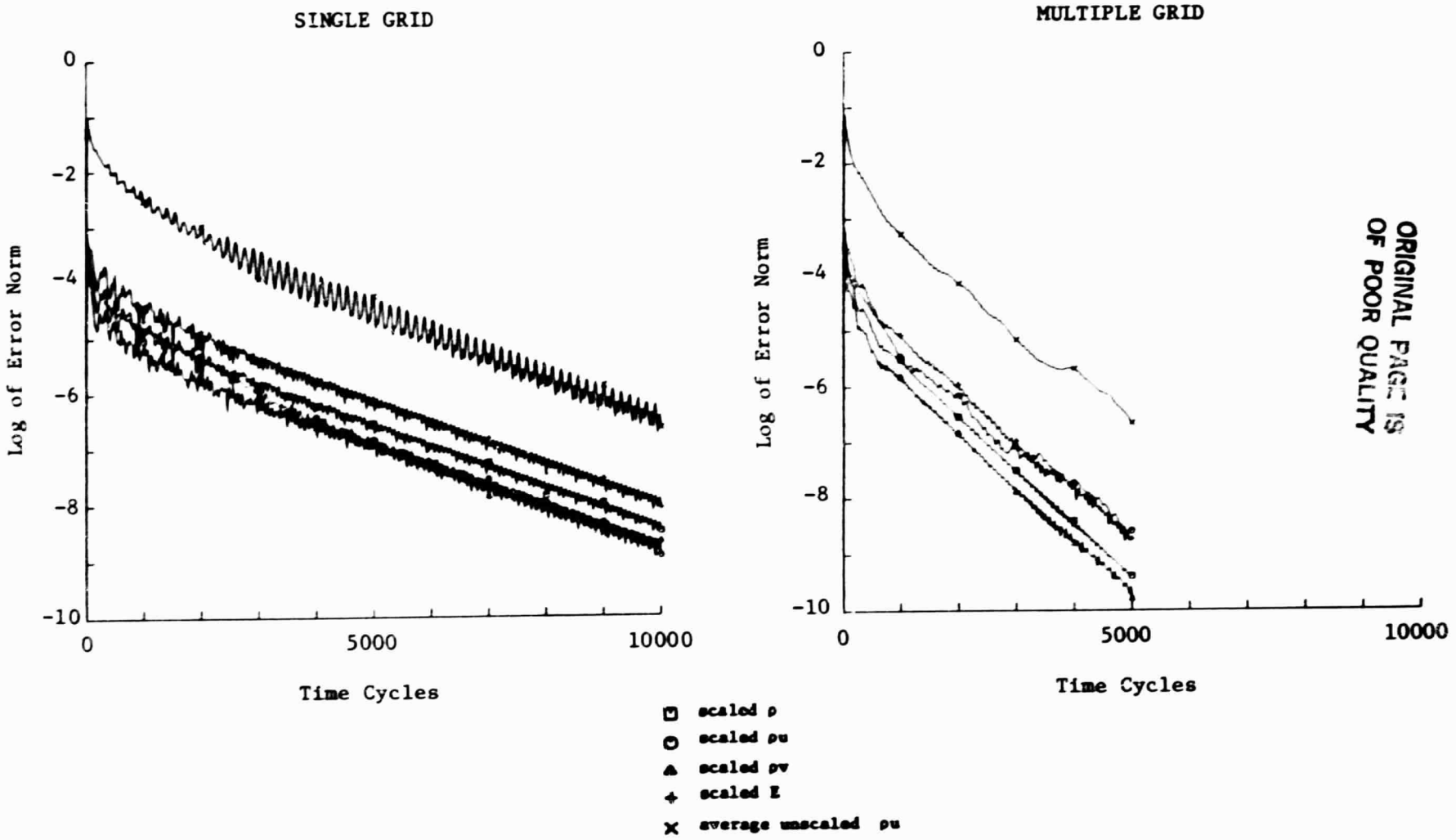




FIGURE 8d. - Convergence Histories

$Re = 3.4 \times 10^4$ $\Delta y = 0.0025$

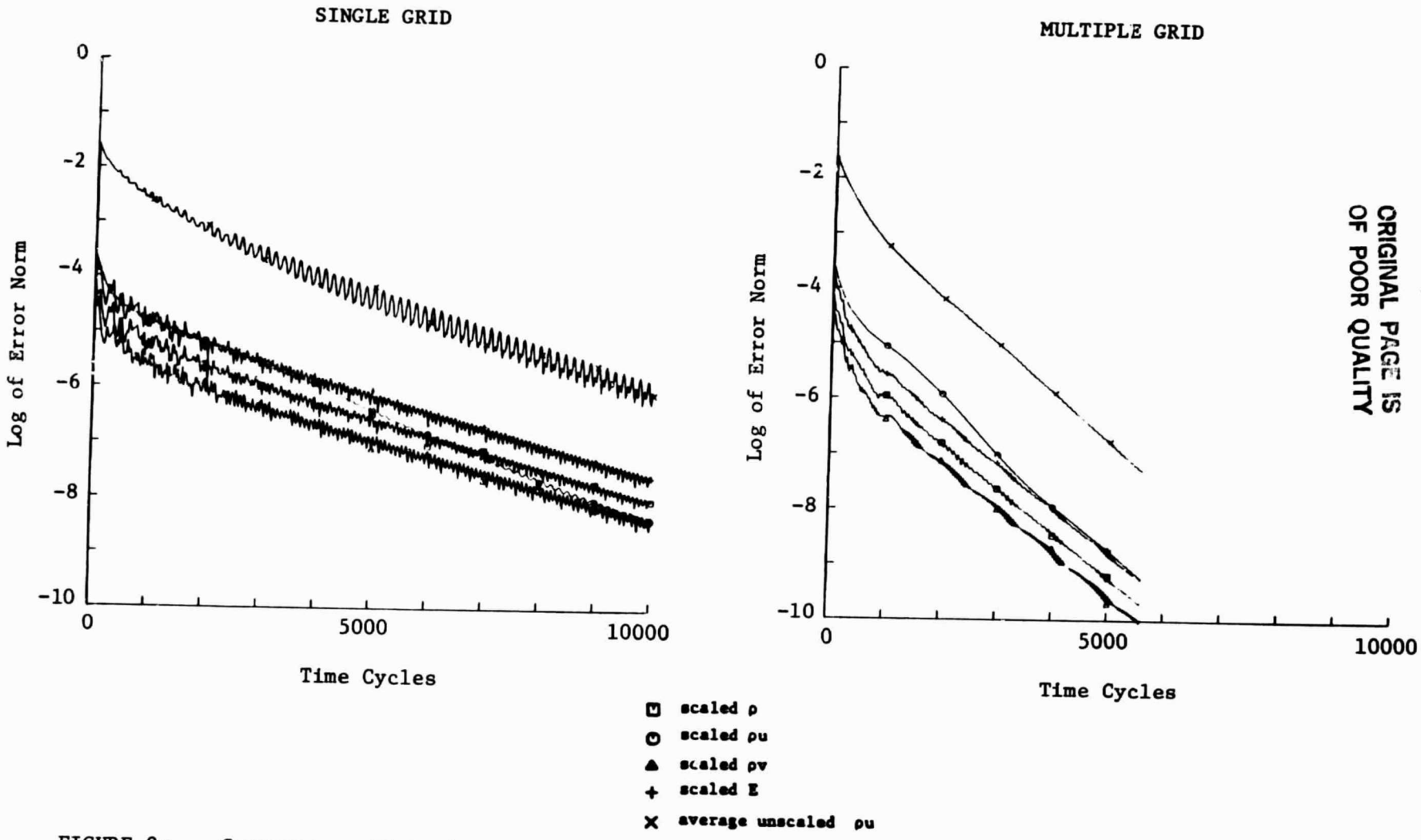




FIGURE 8e. - Convergence Histories

$Re = 2.0 \times 10^5$ , $\Delta y = 0.0025$